Journal of Agricultural Science and Technology B 4 (2014) 731-743
Earlier title: Journal of Agricultural Science and Technology, ISSN 1939-1250
doi: 10.17265/2161-6264/2014.09.006

Understanding the Function of Rays and Wood Density on Transverse Fracture Behaviour of Green Wood in Three Species

Seray Ozden[1] and Anthony Roland Ennos[2]

1. Faculty of Life Sciences, University of Manchester, Manchester M13 9PL, UK

2. School of Biological, Biomedical and Environmental Sciences, University of Hull, Hull HU6 7RX, UK

Received: September 2, 2014 / Published: September 20, 2014.

Abstract: In recent years, there has been an increasing interest in wood properties, because wood is a commonly used and advanced building material. In this paper, the effect of anatomical characters on the transverse fracture properties of green wood was investigated. The specific fracture energy (G_f J/m^2) of ash (*Fraxinus excelsior*), cherry (*Prunus avium*) and birch (*Betula pendula*) was evaluated using double edge notched tensile tests. The tests were performed on both earlywood (EW) and latewood (LW) zones in both the radial-tangential (RT) and the tangential-radial (TR) crack propagation systems. Wood anatomy and the failure patterns of each species were also investigated using environmental scanning electron microscopy (ESEM) and light microscopy (LMC). The results showed that the G_f of RT fracture systems was around 1.5 times greater than in the TR one, whereas there were no significant differences between EW and LW zones. ESEM micrographs showed that the RT fracture system had a rougher fracture surface, while the TR had a nearly smooth and flat fracture surface. In particular, the wood of *F. excelsior* was the toughest, because of its greater percentage of rays and homogenous distribution of ray cells, while *P. avium* and *B. pendula* showed a lower G_f due to their smaller percentage of rays with a distinctive arrangement of ray cells.

Key words: Green wood, fracture energy, rays, transverse failure.

1. Introduction

Wood has been a frequently used material due to its excellent mechanical properties (low density, but high toughness as well as high strength and stiffness, both in tension and compression). The toughness is the fracture mechanical property of wood that is best described as the ability of a material to absorb energy and resist cracking propagation before it fractures [1].

Wood is a sophisticated material with anisotropic behaviour in three main directions: longitudinal (L), radial (R) and tangential (T) [2]. It is composed of cells which have different arrangements, sizes and numbers and each cell type has a key role in sustaining vital functions: vessels, tracheids and fibres are longitudinally orientated; vessels provide water transportation, fibres provide mechanical strength, and tracheids provide both. The rays are also radially oriented, which provides radial reinforcement to the stem [3-11]. This complex structure makes the toughness properties of wood more complicated compared to homogeneous materials; fracture has to proceed through the cells and therefore, the degree of deformation and location of the cell wall plays an important role in characterizing the fracture toughness of wood [12-18].

Cell wall failure may occur in several ways when a sample is loaded by tensile stresses: it may fail between cell walls (interwall, Fig. 1a), across the cell

Corresponding author: Seray Ozden, Ph.D. student, research fields: plant biomechanics, plant anatomy, forestry, wood mechanics, wood anatomy, and trees. E-mail: seray.ozden@manchester.ac.uk.

wall (transwall, Fig. 1b), or within the cell wall (intrawall, Fig. 1b) [12, 18].

One major problem with determining the fracture characteristics of wood is that there are many factors that can affect it: the direction of crack growth, the specimen geometry and size, the load-displacement curve, the maximum load, the anatomy and the test method chosen [19, 20]. To date, several methods have been used on a range of tree species in order to determine the toughness properties of wood [16-34]. Despite this, there are no specific standard test procedures or specimen dimensions for measurements of toughness.

The direction of crack growth is one of the main factors that need to be taken into account when measuring the toughness of wood. There are six main different crack propagation systems. These directions have been expressed by letter abbreviations for the main directions: longitudinal-radial (LR), longitudinal-tangential (LT), radial-longitudinal (RL), radial-tangential (RT), tangential-radial (TR), and tangential-longitudinal (TL) (Fig. 2). The first letter indicates the direction normal to the crack plane and the second letter indicates the direction of crack propagation [21, 28].

The LR and LT directions have not been the main focus of studies of the fracture mechanics of wood due to the complexity of their fracture. It is difficult to carry out experiments across the grain because it has excellent mechanical strength, stiffness and toughness [22, 29, 32, 35]. Jeronimidis [22] found that wood was extremely tough when cut across the grain because this absorbed huge amounts of energy as the cells buckle and the cellulose fibres unwind. In experiments based on extending cracks, the crack cannot find a way along a potential plane of weakness because the fibre cells form a barrier that stops crack growth.

So far, several fracture mechanics studies have focused on the RL and TL systems. Crack propagation occurs parallel to the wood grain in the TL and RL

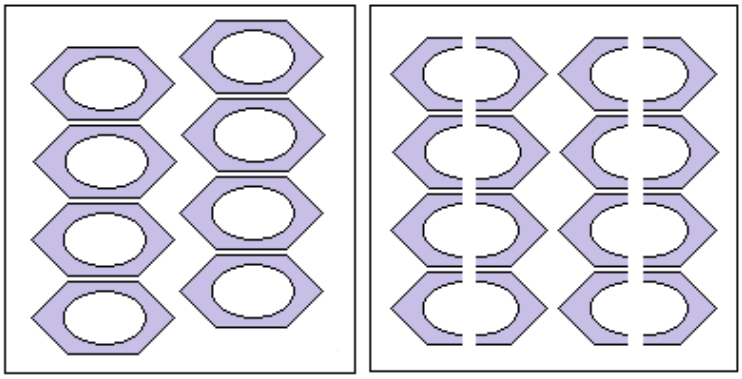

Fig. 1 The failure types of cells: (a) cell separations (interwall) and (b) cell wall fractures (intrawall or transwall).
Source: adopted from Ref. [18].

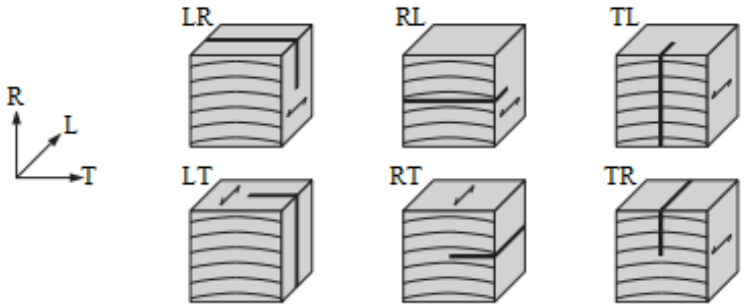

Fig. 2 Wood anatomic axis and fracture systems in wood: longitudinal (L), radial (R) and tangential (T) directions.
Source: adopted from Ref. [33].

directions. A number of researchers have reported that RL toughness is generally higher than TL [3, 8-9, 19, 21-24].

However, few studies have examined the fracture properties in the RT and TR directions [19, 21, 29, 36-39]. Previous studies have reported that toughness is higher in the RT direction than TR directions [21, 39]. However, Schniewind and Centeno [29] did not find a difference in toughness between the RT and TR directions, and surprisingly Nairn [19] found TR toughness was higher than RT toughness.

The RT and TR systems have been mostly ignored, possibly because wood is anisotropic and inhomogeneous in the transverse surface, consisting as it does of both earlywood (EW) and latewood (LW） zones. The mechanical properties should be different in the EW and LW because of their anatomical structure; typically EW has cells with a large lumen and a thin wall, giving a low density, whereas LW has cells with a smaller lumen and thicker walls, giving a high density [21]. Density is the main determinant factor for the mechanical properties of wood [34]. Because the density of LW is higher than the EW, the stiffness and strength tend to be around twice as great in the LW zone, but there is no clear information with regard to whether or not the density has an important role for toughness. Therefore, it is unclear whether the fracture type and mechanical properties of wood should show variation between the EW and LW zones. Ashby et al. [21] observed the fracture behaviour of wood on the transverse surface, comparing their EW and LW zones. They suggested that the fracturing of the EW is characterized by cell wall ruptures, while LW fracturing arises from cell wall peeling [14, 21, 24]. Tukiainen and Hughes [36] also investigated the fracture properties of softwoods between green and dry states in the RT direction: dry samples had mostly the transwall failure behaviour, while green samples appeared to show intercellular fracture.

Furthermore, there are a quite few research studies on the effect of rays on the transverse fracture properties of green wood. Reiterer et al. [8, 9] studied the influence of rays on the fracture properties of dry wood in both RL and TL directions. Their analysis revealed that the RL direction was reinforced by more rays and had a greater G_f than the TL direction. Similarly, the research study by Burgert et al. [10, 11] also found that rays had a more positive impact on the radial strength of green wood than the tangential direction.

The aim of this study was to examine the influence of wood anatomy (i.e., ray characteristics, density and porosity) on the transverse fracture properties of green wood. The failure patterns and wood anatomy of each species were determined using environmental scanning electron microscopy (ESEM) and light microscopy (LMC). On the other hand, double edge notched tensile tests were carried out to investigate G_f (J/m^2) of three green wood species, ash (*F. excelsior*), cherry (*P. avium*) and birch (*B. pendula*) in the RT and TR fracture systems. Trees were selected to have ring-porous (*F. excelsior*) and diffuse-porous (*P. avium* and *B. pendula*) structures.

2. Materials and Methods

2.1 Test Specimens

Clear sapwood test samples were cut from three species of hardwood trees for this experiment: common ash (*F. excelsior*), silver birch (*B. pendula*), and wild cherry (*P. avium*). The first is a ring-porous species and the others are diffuse-porous. Each tree was divided into EW and LW positions separately to identify their G_f results. For each species 60 samples were made, so that 15 tests could be performed in both directions and in both positions of wood, thus tests were performed on a total of 180 samples. The samples were green woods taken from the University of Manchester’s arboretum at Jodrell Bank. The woods were kept in a cold room at 4 °C in plastic bags and kept wet until tests were carried out.

2.2 Tensile Tests

Wood samples were taken from 20-30 cm diameter trunks of trees from the University's Jodrell Bank Arboretum, Cheshire, and were then cut into 5 mm thick wood discs. The discs were then cut into small specimens in both RT and TR directions. Samples were rectangular in shape, being 60 mm in length (*l*), 15 mm in width (*w*) and 5 mm thick (*b*). Each specimen was sanded before tensile tests were performed. Initial notches (*a*) (around 5 mm long) were first produced from either side of the specimens using a double edged razor blade (0.10 mm thick) leaving an uncut ligament length (*lig*) of around 5 mm (Fig. 3). This stopped accidental cleaving, which was a particular problem in the brittle wood samples. These initial notches were made in either the EW or LW position of a sample. To give dependable test results, the orientation of annual growth rings was chosen carefully in regard to the pull direction. The annual ring numbers and growth ring widths were recorded for each specimen. The annual rings were classified according to the specimens' growth ring numbers, which ranged between 2 to 9. Some specimens had wide growth rings and some of them narrow rings.

All tensile tests were carried out on an Instron Universal Testing Machine (model 4301) with a load cell of 1 kN controlled by the series IX software program. The samples were saturated with water in an airtight box for 2 d to 3 d to provide 100% moisture content in the each specimen. Before the tests the dimensions of the specimen were measured and recorded. The rectangular shaped test sample was clamped in the jaws of tensile clamps and the specimen was then stretched until it broke at a speed of 3 mm/min while an interfaced computer recorded the force required. The displacement was obtained by crosshead motion of the machine. The machine ensured no sliding between the specimen and the gripping system because the jaw faces had a coarse tooth pattern which bit tightly into the specimens. At the same time, the computer calculated the total work (W_f) under the load-displacement curve. Then, G_f was calculated by dividing this work by the area of the ligament (A_{lig}) (Eq. (1)):

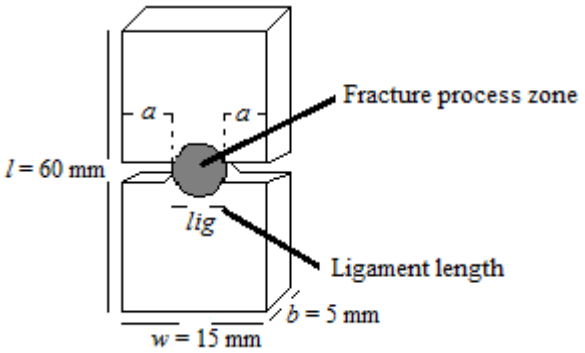

Fig. 3 Demonstrating the geometry and dimensions of test specimen.

$$G_f = \frac{W_f}{A_{lig}} \quad (1)$$

2.3 Anatomical Measurements

2.3.1 Density Measurements

To measure the wood density of each species, rectangular shaped specimen which had 5 × 15 × 60 mm dimensions were used. Additionally the densities of EW and LW zones were measured separately by taking small pieces from these zones, making specimens of variable size. Samples used in EW measurements were obtained from the light coloured part of the growth ring, which has large diameter cells; for LW measurements, samples were collected from the dark coloured area of the growth ring which has small diameter cells. The small EW and LW position samples were cut using a razor blade.

Tested specimens were held in water in airtight containers to provide 100% moisture content for 2 d or 3 d. This approximates the situation of wood within the living tree. The density of each species was then measured. To determine the volume of each sample, it was submerged in a beaker of water standing on an electronic weighing balance and the increase of weight was measured, this being the weight of water displaced by the wood sample. Failure samples were then placed in an oven at 65 °C for 2-3 d until they

had a consistent weight. To determine relative densities for each species, the dry mass of wood is divided by its fresh volume.

2.3.2 ESEM and LMC

Fracture surfaces of each wood species were then examined using an ESEM. The ESEM investigations were carried out on small test samples (5 mm × 15 mm × 60 mm) that were prepared in the RT and TR directions to show failure in both the EW and LW zones. This would allow us to evaluate the effect of wood anatomy on the fracture process and compare the process of fracture in different directions and growth zones. To provide good resolution, samples were coated with gold in a sputter coater. The maximum operating voltage was adjusted to 15 kV for imaging. It was possible to determine fracture properties of small samples at up to 5,000 × magnification using this method.

To determine the characteristics of rays—ray height, ray width, ray number, and volume fraction of ray cells, five microscopic slides were prepared for each species. The specimens were prepared to be less than 1.4 cm long and 0.6 cm wide on the RT surfaces. The sections were photographed and characterised using a Leica MZ95 stereo microscope equipped with Leica Application Suite (LAS) Computer Image Analysis Software. Observations were made at the maximum 60 × magnification to provide better cell photographs. Once the fracture surface was photographed, the sizes and areas of cells could be measured with different measurement tools. In RT specimens, ray width was calculated based on counting the number of cells using analysis software; and ray height was measured using a vector line tool by drawing a line from the top of the ray row to its bottom. We assumed that rays have an elliptical shape and therefore measured the area of rays using the area equation for an ellipse. Finally, the areas of rays were multiplied by their number to calculate the percentage area of rays.

2.4 Statistical Analysis

G_f and density measurements were analysed using one-way and two-way ANOVA and regression analysis using the SPSS Statistics Version 20 at the 5% significance level.

3. Results

3.1 Tensile Test Results

The G_f for the different tree species in the different directions and different growth positions are shown in Fig. 4, and reveal contrasting behaviour. In general, *F.*

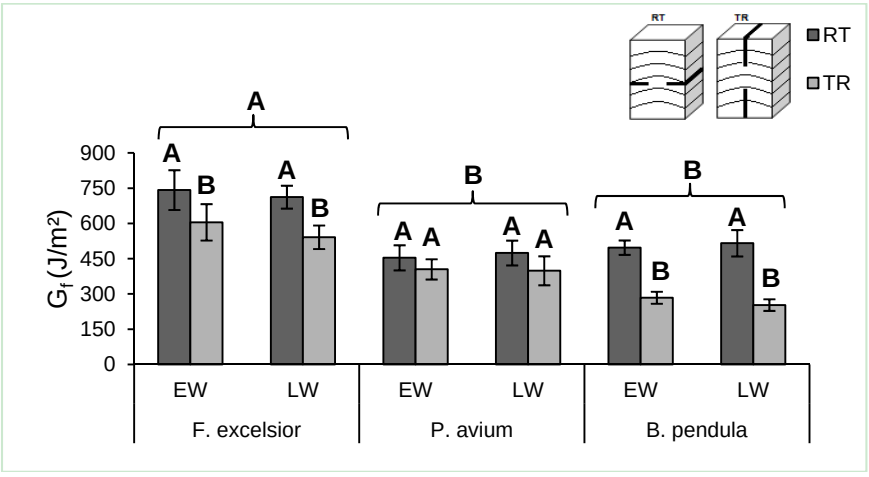

Fig. 4 The G_f for three hardwood tree species.

F. *excelsior* (n = 60), *P. avium* (n = 60) and *B. pendula* (n = 60) calculated from tensile tests in the RT and TR systems and through EW and LW. Error bars represent standard error. Results of post hoc Tukey tests are denoted using letters; within species and between species columns labelled with the same letter present no significant difference and values with different letters show a statistically significant difference at $P < 0.05$.

excelsior was the toughest wood, and G_f was higher in the RT than the TR direction in all woods. Further to these, the difference between directions, "degree of anisotropy", differed between three species; in particular *B. pendula* showed the greatest difference between the RT and TR directions (anisotropy), and *P. avium* the least.

Two-way ANOVA tests were performed for all three hardwood species to determine the effect of direction (RT vs. TR) and the positions of the crack propagation (EW vs. LW breaking) on the G_f in each species. In *F. excelsior* there were significant effects of direction on G_f values ($F_{1, 56}$ = 5.26, P = 0.026), but no significant effect was found for crack position (P > 0.05); in *B. pendula* samples, direction had a significant effect ($F_{1, 56}$ = 42.26, P = 0.000), but not the positions of the crack (P > 0.05); and in *P. avium* neither direction nor the position of the crack had a significant effect (P > 0.05). In *F. excelsior*, G_f was significantly higher in the RT direction than the TR direction (P = 0.000) and the G_f of *B. pendula* was more than double in the RT direction than the TR direction (greatest degree of anisotropy); but the G_f of *P. avium* did not show a significant difference between the RT and TR directions (P > 0.05).

A two-way ANOVA was also performed, with wood species and direction being the factors. This demonstrated that the different species had significantly different G_f ($F_{2, 168}$ = 27.27, P = 0.000) and direction also had a significant effect on G_f properties ($F_{1, 168}$ = 23.82, P = 0.000). Overall, the mean G_f values in the RT direction were higher than in the TR direction. Tukey post hoc tests showed that *F. excelsior* had a significantly higher mean G_f than *P. avium* (P = 0.000), and *B. pendula* (P = 0.000), but there were no significant differences between *P. avium* and *B. pendula* (P > 0.05). The mean G_f of *F. excelsior* was, on average around 1.5 times greater than that of both *P. avium* and *B. pendula*.

3.2 Load-Displacement Diagrams of Three Wood Species

The load-displacement curves of *F. excelsior*, *P. avium* and *B. pendula* species obtained from double edge notched tensile test were examined in detail in order to give further information about their fracture behaviour.

Based on the load-displacement curves (Fig. 5), there were clear differences in the fracture behaviour of the wood species in both the RT and TR systems. The load-displacement curve of *F. excelsior* had a relatively high initial slope during the propagation of the crack which advanced stably with semi-brittle fracture behaviour. In particular, in the RT fracture system, the force rose to break the sample, then fell slowly after reaching a peak. In contrast, in *P. avium*, the cracks propagated unstably and the load decreased rapidly with a brittle fracture behaviour (Fig. 5); *B.*

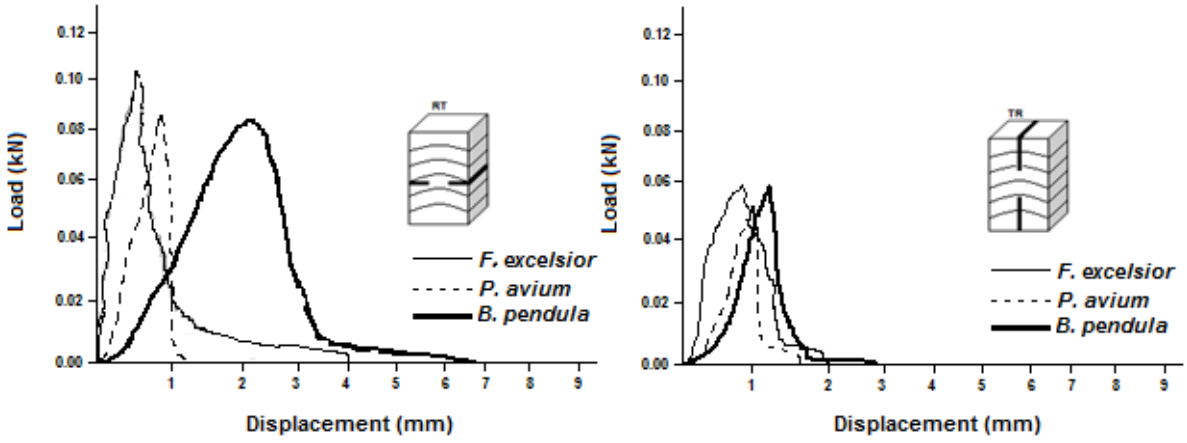

Fig. 5 The load-displacement curves of three hardwood species in the RT and TR directions.

pendula showed a particularly marked contrast to fracture failure behaviour between the RT and TR systems; it fell rapidly to zero with low energy consumption in the TR system, while the RT fracture had a far slower drop after the maximum force had been reached, showing very high energy absorption.

These observations correlate with the greater G_f in both *F. excelsior* and especially *B. pendula* in the RT direction, and the more brittle failure of *P. avium* and all wood in the TR system.

3.3 Density Results

The three hardwood species: *F. excelsior*, *P. avium* and *B. pendula* had growth rings of contrasting width. Growth rings were approximately 8-9 mm wide in *F. excelsior*, and 5-6 mm in *P. avium* and *B. pendula*. The densities of the wood samples from EW and LW are shown in Fig. 6. It can be seen that in all three species EW was less than half as less dense as LW. A two way ANOVA investigating the effects of species and position showed that LW was significantly denser than EW ($F_{1, 84} = 724.89$, $P = 0.000$) and the presence of LW was significantly different between species ($F_{2, 42} = 11.67$, $P = 0.000$) so the percentage of LW in *F. excelsior* was greater than that in both *P. avium* and *B. pendula*. Tukey post hoc tests showed that the percentage of LW was different between each species: there were significant differences between *F. excelsior* and *P. avium* ($P = 0.000$), and *F. excelsior* and *B. pendula* ($P = 0.000$), but there were no significant differences between *P. avium* and *B. pendula* ($P > 0.05$). In contrast to LW, the percentage of EW did not show significant differences between species ($P > 0.05$).

The density measurements taken from failure samples for the crack positions of EW vs. LW and crack directions of RT vs. TR showed a similar difference between species. A two-way ANOVA was performed with species and position being the two factors. This revealed that there were significant differences between the three hardwood species ($F_{2, 168} = 21.84$, $P = 0.000$). Tukey post hoc tests showed that the densities were significantly different in each species: *F. excelsior* had significantly denser wood than *P. avium* ($P = 0.015$) and *B. pendula* ($P = 0.000$); and also *B. pendula* had higher density than *P. avium* ($P = 0.000$). *F. excelsior* had the densest wood with a mean density of 0.53 g/cm^3 followed by *B. pendula* at 0.51 g/cm^3 and *P. avium* at 0.49 g/cm^3.

3.4 Anatomical Measurements of Rays

A one-way ANOVA indicated that the average area of rays was significantly different between three species (Fig. 7a) ($F_{2, 12} = 40.20$, $P = 0.000$); a post hoc

Fig. 6 The densities of EW and LW zones in three different hardwood species.
F. *excelsior* ($n = 30$), *P. avium* ($n = 30$) and *B. pendula* ($n = 30$). Error bars represent standard error. Results of post hoc Tukey tests are denoted using letters; within species and between species columns labelled with the same letter present no significant difference and values with different letters show a statistically significant difference at $P < 0.05$.

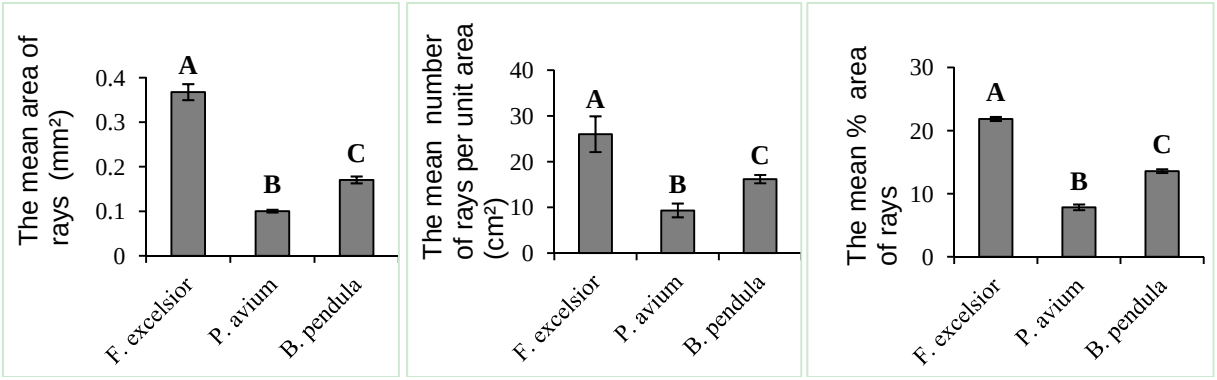

(a) (b) (c)

Fig. 7 (a) The average area of rays, (b) the mean number of rays per unit area and (c) the mean % area of rays for three wood species.

All groups $n = 5$. Error bars represent standard error. Results of post hoc Tukey tests are denoted using letters; between species columns labelled with the same letter present no significant difference and values with different letters show a statistically significant difference at $P < 0.05$.

Tukey test showed the average area of rays was significantly higher in the wood of *F. excelsior* than that of other two species ($P = 0.000$). From Fig. 7b, it can be seen that there were more rays in *F. excelsior* than *P. avium* and *B. pendula* in the RT sections, and fewer rays in *P. avium*. A one-way ANOVA showed that the mean number of rays per unit area was significantly different between species ($F_{2, 12} = 11.44$, $P = 0.001$). Tukey post hoc tests illustrated that *F. excelsior* had significantly more rays than *P. avium* and *B. pendula* ($P = 0.000$), but there was no significant difference between *P. avium* and *B. pendula* ($P > 0.05$). A one-way ANOVA was also performed in % area of rays in each species indicating that there were significant differences between species ($F_{2, 12} = 375.71$, $P = 0.000$) (Fig. 7c). Tukey post hoc tests showed that all species had significantly different % area of rays ($P = 0.000$). It can be seen in Fig. 7c, the % area of rays of *F. excelsior* was nearly 1.5 times greater than that of the other two species.

4. Discussion

4.1 Clear Pattern of Results for G_f

Both between and within the three hardwood species there were clear differences in fracture behaviour. The results of tensile tests showed that the G_f was significantly greater in the RT fracture surface than TR fracture in all cases. *B. pendula* showed the most anisotropic behaviour followed by *F. excelsior* and then *P. avium*; G_f was nearly two times bigger in the RT direction than the TR direction. *F. excelsior* also had nearly 1.5 times greater G_f in both RT and TR fracture surfaces than that of the other two species and the G_f of *B. pendula* was higher than that of *P. avium* (Fig. 4). These can be explained by the anatomy of the species and to the fracture patterns that resulted.

Our results agree with those of Attack et al. [39] and Ashby et al. [21], which also revealed that toughness was higher in the RT direction than that in the TR direction. Attack et al. [39] studied green wood as we did, and found that green spruce wood had nearly two times higher G_f in the RT direction than that in the TR direction. However, our G_f results for *B. pendula* were lower than those of Koponen and Tukiainen [37] who found the G_f in RT with mean 800.4 J/m^2 in dry wood, whereas the *B. pendula* had mean 506.5 J/m^2 G_f in our study; this was possibly because our specimens were in the green state and had lower density. In contrast, the study by Schniewind and Centeno [29] indicated that toughness did not differ significantly between the RT and TR directions.

In our anatomical measurements, it was clearly seen that the anisotropy was mainly due to rays, namely

most energy was produced to break through them (Fig. 8a). Previous studies have reported that rays act a part as being either fracture stoppers in the RT system or fracture initiators in the TR system [8, 9, 21, 40, 41]. Our fracture pattern observations from ESEM micrographs showed that RT fracture was mostly dominated by transwall or interwall failure (Fig. 8a), whereas TR was a mainly intrawall failure (Fig. 9**)** [8, 9, 21, 29, 42-44]. This agrees with Ashby et al. [21], which revealed that RT direction showed mostly cell breaking during crack propagation, and more cell wall ruptures in the TR direction.

In the RT fracture system the irregular arrangement and hexagonal shape of ray cells functioned as a strengthening contribution to giving more strength and stiffness as well as more toughness than that in the TR direction [45]. The cells are connected with each other like rows of ribs. Consequently, in our experiments when the test samples were stretched in the RT fracture system, the stresses were transferred from cell to cell in the aggregations of rays and this action probably slowed the advance speed of the crack. This rough fracture process proceeded along the cell wall with an extension in the RT system from one cell, spreading to other cells with more energy consumption; therefore the fracture system was seen as rugged and rough (Fig. 8a). In contrast in the TR direction, rays had a negative effect for fracture toughness because rays induce an easy fracture path. When the crack begins to grow, the regular shapes of

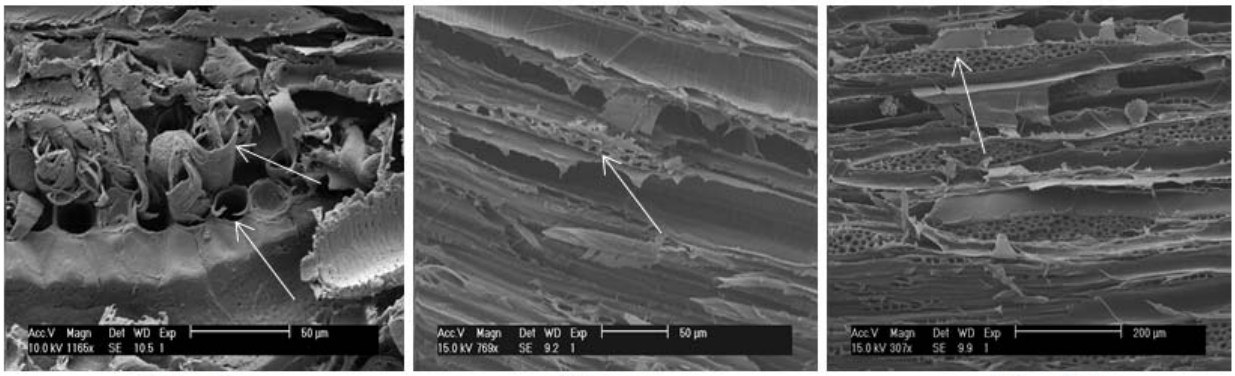

Fig. 8 Demonstrating ESEM micrographs of RT tensile failure patterns in three species.
(a) the RT tensile failure pattern of *F. excelsior* where the ray cells failed; arrows show unwinding that suggests more energy is needed to break cells. (b) the arrangement of rays in the RT crack system for *P. avium*; there appears to be less ductile fracture in the rays. (c) the RT tensile failure pattern of *B. pendula* where the ray cells failed and the cell wall ruptured.

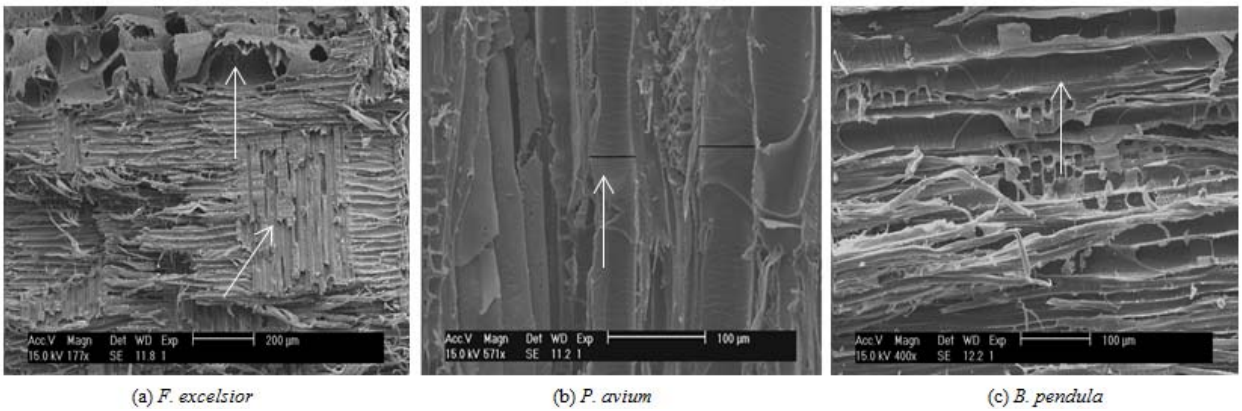

Fig. 9 Demonstrating ESEM micrographs of TR tensile failure patterns in three species.
(a) the failure mode in TR tension of *F. excelsior*; the vessels failed in the EW (top), but in the LW cracks had to run through narrower, thicker-walled fibres. (b) the failure mode in TR tension of *P. avium*; the vessels failed in the EW (centre). (c) the failure mode in TR tension of *B. pendula* where cracks ran between the vessels, which then failed.

rays may act a part as a crack initiator [8, 9, 21, 40, 41]. Thus, rapid fracture occurred and developed more cell deformations with less energy consumption (Fig. 9) during crack propagation.

The greater toughness of *F. excelsior* is probably due to its density and higher percentage of rays. The density of *F. excelsior* was significantly greater than both of the other two species (Fig. 6). Density is known to be the main factor for strength and stiffness of wood. Toughness of wood is also mainly associated with its density. Denser wood has a higher cell wall thickness and so more energy is required to break the cell walls, whereas less dense woods have thinner-walled cells [8, 9, 11, 21, 44-49].

The same results were also verified in our results for *B. pendula* and *P. avium*: *B. pendula* showed the second highest G_f and was the second most dense wood and the G_f in *P. avium* was lowest as was its wood density. Our anatomical measurements also indicated that the percentage of rays were found to be about 1.5 times bigger in *F. excelsior* than *B. pendula* and over twice than that in *P. avium*. So it was no surprise that the wood with the highest G_f had more rays and the highest volume fraction of rays (Figs. 7b and 7c) and thus it was found that there was a positive effect of increasing the volume fraction of rays on G_f because the rays showed a homogenous distribution with sturdy fracture manner. The failure pattern demonstrated in ray cells of *F. excelsior* appeared to involve large numbers of spiral failure and buckling events (Fig. 8a). There was less cell wall deformation and the fracture process used more energy than in the other two species. In contrast to *F. excelsior*, *P. avium* showed more brittle behaviour with a clean fracture because of its lower density and significantly smaller amount of ray cells. The fracture patterns also showed that *P. avium* had more ray cell deformations in both two directions so the crack required great cell deformations and broke with less energy consumption and rapid fracture in the RT as well as in the TR fracture surface (Figs. 8b and 9b). However, interestingly, this is contrary to a study conducted by Mohammadi and Nairn [50]. They found that RT toughness was higher than TR one. They also suggested rays had a negligible reinforcing effect on the RT direction.

However, despite the fact that *B. pendula* had fewer rays and a lower percentage of rays than *F. excelsior*, surprisingly, it showed higher anisotropy as having around two times greater G_f in the RT system than that in the TR system. In addition, there was contrasting fracture behaviour in these directions because RT fracture showed ductile behaviour (Fig. 8c) similar to that in *F. excelsior*, but TR fracture was more brittle (Fig. 9a). The reason for this difference can be also explained by its lower contribution of toughness due to the fibres and vessels.

The lower G_f values of *P. avium* and *B. pendula* might also be due to patterns of porosity because the ring-porous species (*F. excelsior*) exhibited greater fracture resistance than the diffuse-porous ones (*P. avium* and *B. pendula*). This could result from the cell distributions, contributions and sizes because ring-porous woods have a wide variation in cell size between EW (dominated by large cells) and LW regions (dominated by small cells) [21, 36]. In contrast, in diffuse-porous species, here, particularly *P. avium*, the structure was not so complex because the EW and LW regions have the same size cells. Cracks, therefore, travelled through vessels easily in the TR direction because the cracks which run between vessels more easily caused great cell wall deformations due to its more diffuse porosity (Fig. 8a) [21, 43]. This would help explain why *P. avium* and *B. pendula* exhibited a more brittle failure manner, especially in the TR direction.

In contrast, vessels in *F. excelsior* showed less brittle behaviour and were more resistant in the TR fracture surface than vessels in *B. pendula*. In this ring-porous wood the vessels did not line up radially as they did in *B. pendula* because the large vessels were all aligned tangentially along the growth rings.

In ring-porous species the cells were also closely clumped together. When a specimen was exposed to load, a crack would not easily travel between cells. This is because cells were located in rows with narrow void spaces. Crack growth may encounter the LW region, which is mainly comprised of fibre cells and it may not be able to process along the weaker regions [29, 47, 51, 52]. The failure was therefore mainly dominated by both interwall and intrawall failure behaviour and this, seen in vessels in *F. excelsior*, produced more energy consumption (Fig. 9a).

5. Conclusions

Our study showed that the differences in fracture properties of three hardwood species were due to differences in their wood anatomy. In *F. excelsior*, cracks in both directions were characterized by mostly interwall or transwall fracture with more ductile behaviour, while in *B. pendula* the fracture showed significant differences between RT and TR fracture systems because the fracture in RT system was more ductile involving both the interwall and intrawall fracture manner, but the TR system showed great cell wall deformations dominated by intrawall fracture. The fracture in *P. avium* was mainly intrawall failure with cell wall ruptures. The percentage of rays and wood density were found to be the main factors that influenced these differences in fracture behaviour and fracture toughness. Wood with a higher percentage of rays and density resulted in higher values of G_f. In contrast to rays, vessels were the mechanically weak points because they acted as crack initiators.

References

[1] Dinwoodie, J. M. 1981. *Timber: Its Nature and Behaviour*. New York: Van Nostrand Reinhold, 190.

[2] Green, D. W., Winandy, J. E., and Kretschmann, D. E. 1999. "Mechanical Properties of Wood." In *Wood as An Engineering Material.* Madison, Winsoncin: Department of Agriculture, USDA Forest Service, Forest Product Laboratory, 463.

[3] Dinwoodie, J. M. 1975. "Timber—A Review of the Structure-Mechanical Property Relationship." *J. Microsc.* 104 (1): 3-32.

[4] Price, A. T. 1928. "A Mathematical Discussion on the Structure of Wood in Relation to Its Elastic Properties." *Phil. Trans. R. Soc. Lond*. A 228: 1-62.

[5] Markwardt, L. J., and Wilson, T. R. C. 1935. *Strength and Related Properties of Woods Grown in the United States*. Washington: U.S. Government Printing Office, Department of Agriculture Technical Bulletin 479.

[6] Panshin, A. J., and de Zeeuw, C. 1980. *Textbook of Wood Technology*. 4th ed., New York: McGraw-Hill, 722.

[7] Tan, S., Wolfe, G. R., Cunningham, F. X., and Gantt, E. 1995. "Decrease of Polypeptides in the PS I Antenna Complex with Increasing Growth Irradiance in the Red Alga *Porphyridium cruentum*." *Photosynth. Res.* 45: 1-10.

[8] Reiterer, A., Sinn, G., and Stanzl-Tschegg, S. E. 2002. "Fracture Characteristics of Different Wood Species under Mode I Loading Perpendicular to the Grain." *Materials Science and Engineering* A 332 (1-2): 29-36.

[9] Reiterer, A., Burgert, I., Sinn, G., and Tschegg, S. 2002. "The Radial Reinforcement of the Wood Structure and Its Implication on Mechanical and Fracture Mechanical Properties—A Comparison between Two Tree Species." *Journal of Materials Science* 37 (5): 935-40.

[10] Burgert, I., Bernasconi, A., and Eckstein, D. 1999. "Evidence for the Strength Function of Rays in Living Trees." *Holz als Roh- und Werkstoff* 57 (5): 397-9.

[11] Burgert, I., Bernasconi, A., Niklas, K. J., and Eckstein, D. 2001. "The Influence of Rays on the Transverse Elastic Anisotropy in Green Wood of Deciduous Trees." *Holzforschung* 55 (5): 449-54.

[12] River, B. H., Vick, C. B., and Gillespie, R. H. 1991. "Wood as an Adherend." In *Treatise on Adhesion and Adhesives*, edited by Minford, J. D. Vol. 7, New York: Marcel Dekker, 230.

[13] Wardrop, A. B., and Addo-Ashong, F. W. 1963. "The Anatomy and Fine Structure of Wood in Relation to Its Mechanical Failure." In *Proceedings of the Second Tewksbury Symposium on Fracture*, 169-200.

[14] Koran, Z. 1967. "Electron Microscopy of Radial Tracheid Surfaces of Black Spruce Separated by Tensile Failure at Various Temperatures." *Tappi* 50 (2): 60-7.

[15] Koran, Z 1968. "Electron Microscopy of Tangential Tracheid Surfaces of Black Spruce Separated by Tensile Failure at Various Temperatures." *Svensk Papperstidning* 17: 568-76.

[16] DeBaise, G. R. 1970. "Mechanics and Morphology of Wood Shear Fracture." Ph.D thesis, State University College of Forestry, Syracuse University, Syracuse, New York.

[17] DeBaise, G. R. 1972. "Morphology of Wood Shear

Fracture." *Journal of Materials* 7 (4): 568-72.

[18] Cote, W. A., and Hanna, R. B. 1983. "Ultrastructural Characteristics of Wood Fracture Surfaces." *Wood Fiber Sci.* 15 (2): 135-63.

[19] Nairn, J. A. 2007. "Material Point Method Simulations of Transverse Fracture in Wood with Realistic Morphologies." *Holzforschung* 61: 375-81.

[20] Tschegg, E. K. 1986. Equipment and appropriate specimen shape for tests to measure fracture values. Patent AT-390328. (in German)

[21] Ashby, M. F., Easterling, K. E., Harrysson, R., and Maiti, S. K. 1985. "The Fracture and Toughness of Woods." *Proc. R. Soc. Lond.* A 398: 261-80.

[22] Jeronimidis, G. 1980. "The Fracture Behaviour of Wood and the Relations between Toughness and Morphology." *Proc. R. Soc. Lond.* B 208: 447-60.

[23] Lucas, P. W., Tan, H. T. W., and Cheng, P. Y. 1997. "The Toughness of Secondary Cell Wall and Wood Tissue." *Phil. Trans. R. Soc. Lond.* B 352: 341-52.

[24] Petterson, R. W., and Bodig, J. 1982. "Prediction of Fracture Toughness of Conifers." *Wood Fiber Sci.* 15 (4): 302-16.

[25] Bostrom, L. 1994. *Machine Strength Grading, Comparison of Four Different Systems*. SP report, SP Swedish National Testing and Research Institute, Boras, Sweden.

[26] Wu, E. M. 1967. "Application of Fracture Mechanics to Anisotropic Plates." *J. Appl. Mech.* 34: 967-74.

[27] Schniewind, A. P., and Pozniak, R. A. 1971. "On the Fracture Toughness of Douglas Fir Wood." *Engineering Fracture Mechanics* 2 (3): 223-33.

[28] Walsh, P. F. 1972. "Linear Fracture Mechanics on Orthotropic Materials." *Engineering Fracture Mechanics* 4: 533-41.

[29] Schniewind, A. P., and Centeno, J. C. 1973. "Fracture Toughness and Duration of Load Factor I: Six Principal Systems of Crack Propagation and the Duration Factor for Cracks Propagating Parallel to Grain." *Wood Fiber* 5: 152-9.

[30] Barrett, J. D. 1981. "Fracture Mechanics and the Design of Wood Structures." *Phil. Trans. R. Soc. Lond.* A 299: 217-26.

[31] De Moura, M. F. S. F., Oliveira, J. M. Q., Morais, J. J. L., and Xavier, J. M. C. 2010. "Mixed-Mode I/II Wood Fracture Characterization Using the Mixed-Mode Bending Test." *Engineering Fracture Mechanics* 77: 144-52.

[32] Tattersall, H. G., and Tappin, G. 1966. "The Work of Fracture and Its Measurements in Metals, Ceramics and Other Materials." *J. Mater. Sci.* 1: 296-301.

[33] Danielsson, H. 2013. "Perpendicular to Grain Fracture Analysis of Wooden Structural Elements Models and Applications." Ph.D. thesis, Lund University, Sweden.

[34] Stanzl-Tschegg, S. E., and Navi, P. 2009. "Fracture Behaviour of Wood and Its Composites. A review COST Action E35 2004-2008: Wood Machining-Micromechanics and Fracture." *Holzforschung* 63 (2): 139-49.

[35] Robinson, W. 1920. "The Microscopical Features of Mechanical Strains in Timber and the Bearing of These on the Structure of the Cell Wall in Plants." *Phil. Trans. R. Soc. Lond.* B 210: 49-82.

[36] Tukiainen, P., and Hughes, M. 2013. "Fracture Behaviour of Birch and Spruce in RT-Direction in Mesoscale." *Holzforschung* 67 (6): 673-81.

[37] Koponen, S., and Tukiainen, P. 2006. "Fracture Behaviour and Cutting of Small Wood Specimens in RT Direction." In *Fracture of Nano and Engineering Materials and Structures*, edited by Gdoutos, E. E. Netherlands: Springer.

[38] Vasic, S., and Stanzl-Tschegg, S. E. 2007. "Experimental and Numerical Investigation of Wood Fracture Mechanisms at Different Humidity Levels." *Holzforschung* 61: 367-74.

[39] Attack, D., May, W. D., Morris, E. L., and Sproule, R. N. 1961. "The Energy of Tensile and Cleavage Fracture of Black Spruce." *Tappi* 8: 555-67.

[40] Dresch, H. E., and Dinwoodie, J. M. 1996. *Timber: Structure, Properties, Conversion and Use.* 7th ed., Binghamton, NY: Haworth Press, 306.

[41] Bowyer, J. L., Shmulsky, R., and Haygreen, J. G. 2003. *Forest Products and Wood Science: An Introduction.* 4th ed., Ames, Iowa, USA: Blackwell Publishing.

[42] Delorme, A., and Verhoff, S. 1976. "Cell Wall Deformation in Norway Spruce Due to Damage by Storms, as Revealed by Scanning Electron Microscopy." *Holz als Roh- und Werkstoff* 33: 456-60.

[43] Keith, C. T., and Cote, W. A. Jr. 1968. "Microscopic Characterization of Slip Lines and Compression Failures in Wood Cell Walls." *Forest Products Journal* 18 (3): 67-74.

[44] Bodner, J., Schlag, M. G., and Grüll, G. 1997. "Fracture Initiation and Progress in Wood Specimens Stressed in Tension—Part I: Clear Wood Specimens Stressed Parallel to the Grain." *Holzforschung* 51: 479-84.

[45] Kahle, E., and Woodhouse, J. 1994. "The Influence of Cell Geometry on the Elasticity of Softwoods." *J. Mater. Sci.* 29 (5): 1250-9.

[46] Gibson, L. J., and Ashby, M. F. 1988. *Cellular Solids: Structure and Properties.* Oxford: Pergamon Press.

[47] Ifju, G. 1964. "Tensile Strength Behaviour as a Function of Cellulose in Wood." *Forest Products Journal* 14 (8): 366-72.

[48] Schachner, H., Reiterer, A., and Stanzl-Tschegg, S. E. 2000. "Orthotropic Fracture Toughness of Wood." *J.*

Mater. Sci. Lett. 19: 1783-5.

[49] Thuvander, F., Jernkvist, L. O., and Gunnars, J. 2000. "Influence of Repetitive Stiffness Variation on Crack Growth Behaviour in Wood." *J. Mat. Sci.* 35: 6259-66.

[50] Mohammadi, M. S., and Nairn, J. A. 2014. "Crack Propagation and Fracture Toughness of Solid Balsa Used for Cores of Sandwich Composites." *Journal of Sandwich Structures and Materials* 16 (1): 22-41.

[51] Mark, R., and Gillis, P. P. 1970. "New Models in Cell-Wall Mechanics." *Wood and Fiber* 2 (2): 79-95.

[52] Kifetew, G., Thuvander, F., Berglund, L., and Lindberg, H. 1998. "The Effect of Drying on Wood Fracture Surfaces from Specimens Loaded in Wet Condition." *Wood Science and Technology* 32: 83-94.